Reliability Analysis of an Ultrasonic Guided Wave Based Structural Health Monitoring System for a Carbon Fibre Reinforced Thermoplastic Torsion-box

Ochoa, Pedro; Groves, Roger; Benedictus, Rinze

Publication date
2017

Document Version
Accepted author manuscript

Published in
Structural Health Monitoring 2017: Real-Time Material State Awareness and Data-Driven Safety Assurance - Proceedings of the 11th International Workshop on Structural Health Monitoring, IWSHM 2017

Citation (APA)
Ochoa, P., Groves, R., & Benedictus, R. (2017). Reliability Analysis of an Ultrasonic Guided Wave Based Structural Health Monitoring System for a Carbon Fibre Reinforced Thermoplastic Torsion-box. In F. K. Chang, & F. Kopsaftopoulos (Eds.), *Structural Health Monitoring 2017: Real-Time Material State Awareness and Data-Driven Safety Assurance - Proceedings of the 11th International Workshop on Structural Health Monitoring, IWSHM 2017* (Vol. 2, pp. 1708-1714). Destech publications.

Important note
To cite this publication, please use the final published version (if applicable).
Please check the document version above.

Title: Reliability analysis of an ultrasonic guided wave based structural health monitoring system for a carbon fibre reinforced thermoplastic torsion-box

Authors: Pedro Ochôa
Roger M. Groves
Rinze Benedictus

ABSTRACT

Certification is the key step towards the implementation of structural health monitoring (SHM) as part of condition based maintenance programmes of aircraft fleets. That can only be accomplished by demonstration of system performance in multiple scenarios and in a statistically relevant way. This paper describes a fully computational approach for reliability assessment of an ultrasonic guided wave (GW) based SHM system for a full-scale stiffened panel of a horizontal stabilizer torsion-box entirely made of carbon fibre reinforced thermoplastic. A pseudo-stochastic nature is attributed to the damage index values calculated from the finite-element signals, allowing hit-miss data to be generated. That data is in turn employed for the computation of probability of detection curves and relative operating characteristics. The results of this research show that detailed damage diagnostics in full-scale complex composite structures can be achieved by using ultrasonic GWs under the hot-spot monitoring philosophy. Moreover, it is demonstrated that properly validated models of the monitoring environment can be used for reliability analysis of GW based SHM systems for full-scale complex composite structures, thereby reducing the need for extensive and costly experimental test campaigns, which in turn can contribute to an acceleration of the establishment of a certification framework for SHM systems.

INTRODUCTION

In the last two decades it has been demonstrated that ultrasonic guided waves (GW) have a high potential for detailed quantitative damage diagnostic in thin composite structures [1 - 9]. However, the main aircraft manufacturers claim that the lack of robust characterization of structural health monitoring (SHM) systems in representative environments is still preventing their certification and implementation

---

Pedro Ochôa, Roger M. Groves and Rinze Benedictus, Delft University of Technology, Faculty of Aerospace Engineering, Structural Integrity and Composites Group, Kluyverweg 1 (building 62), 2629 HS, Delft, The Netherlands.

as part of condition based maintenance programmes [10]. Contrary to non-destructive testing techniques [11, 12], no standard methods have been established for reliability quantification of SHM systems, mostly because the transducers are not movable. That apparently simple constraint imposes high monetary and time costs on the experimental certification of such systems since a large number of components would have to be produced, instrumented and tested in order to cover all the possible scenarios in a statistically relevant way [13]. The limited number of acoustic-ultrasonic SHM systems tested in full-scale aircraft primary composite structures until today [10] is representative of these constraints.

This situation has led research on reliability characterisation of ultrasonic SHM systems to consider small planar coupons, either metallic or composite, in order to prevent test campaigns from becoming unfeasible, while adapting and extending the reliability assessment methods traditionally employed in NDT. Cobb *et al*. [14, 15] developed a model-assisted approach to estimate the probability-of-detection (PoD) of fatigue cracks in rectangular aluminium coupons inspected with shear wave transducers. However, their methodology required an extensive experimental database of damage index (DI) values correlated with the observed crack length, which took *"several years"* [14] to be compiled. Being aware of this tedious process, Memmolo *et al*. [16] adopted a fully computational methodology for reliability assessment. They experimentally validated a finite-element (FE) model of GW propagation in a composite plate, which was employed to generate DI data for different scenarios of low-energy impact damage. The numerical DI values were then disturbed by adding Gaussian noise in order to mimic experimental uncertainty. In this way it was possible to create multiple pseudo-stochastic data points for each damage level, thereby enabling hit/miss counting and subsequent PoD curve estimation.

The core issue for fully computational approaches is the accuracy of the simulated monitoring environment. The more accurate the models are, the more one can rely on numerical data sets for the reliability assessment of SHM systems. This was the motivation for Janapati *et al*. [17] to investigate in detail the sensitivity of damage detection to specific intra-measurement variability sources. They took small aluminium coupons with through-thickness cracks at a central hole, and bonded an actuator-sensor piezo-ceramic (PZT) pair on to each of them. A parametric study was conducted with the spectral element method for seven different damage scenarios by varying the PZT material properties, structure material properties and adhesive properties, adhesive thickness, and sensor location. By comparing the numerical and experimental results they were able to establish quantitative correlations between isolated sources of variability and their actual observed effect on the DI, thereby partially characterizing the factors that influence the performance of the transducer network.

Nevertheless, key factors such as geometric complexity, material anisotropy, and transducer network degradation have not been simultaneously taken into account. This study aims precisely at bridging this gap by performing a computational reliability analysis of an ultrasonic GW based SHM system for a full-scale stiffened-panel of a horizontal stabilizer torsion-box entirely made of carbon fibre reinforced thermoplastic. The FE method is employed to simulate the monitoring environment in a wide range of scenarios, where the size of damage, the excitation frequency, and the transducer bonding condition are varied. Numerical DI data is artificially disturbed with a normally distributed error in order to mimic intra-measurement variability. In

turn, this pseudo-stochastic data is used for hit/miss data generation which, ultimately, allows the calculation of probability-of-detection (PoD) in a statistically relevant way.

RELIABILITY ANALYSIS PROTOCOL

A fully computational approach to the reliability analysis of an ultrasonic GW based SHM system must start with the identification of its variability factors. Some of the most important are: A) dimensions of the structure, B) properties of the structure, C) thickness of PZT bonding layer, D) condition of PZT bonding layer, E) signal noise, F) temperature, G) pressure, H) loading, I) type of damage, J) location of damage, K) orientation of damage, L) size of damage, M) position of actuator within the network, N) excitation frequency, O) dimensions of PZT patch, P) properties of PZT material.

For the current study, it was decided to analyse the effect of factors that are directly related to characteristics of the transducer network (D, M, N), together with the effect of damage evolution (L). Factors A-C, O, P are sources of random variability, and their influence is considered to be covered by the study of Janapati *et al*. [17]. The combined effect of factors F to H on wave propagation is mostly felt in the amplitude and instantaneous phase of the sensed signals, which in turn changes the effectiveness of the selected threshold, thereby affecting the performance of the SHM system. Therefore, these factors, together with factor E, can be partially assessed by computing the PoD of the critical damage for several detection thresholds, which can also be referred to relative operating characteristics (ROC) analysis. Factors I to K are associated with damage characteristics which are determinant for the change in ultrasound scattering in the structure. However, in the current study, these parameters are not variable, as they are fixed by the manufacturer in the definition of the *hot-spot* (i.e. critical area/configuration) to be monitored.

The chosen parameters are varied in order to cover the different regimes of operation and damage scenarios. The condition of the PZT bonding layer (factor D) describes the portion of the actuator patch which is effectively bonded to the surface of the structure, and it ranges from ¼ to 1, in steps of ¼. Since the transducer distribution is symmetric with respect to stringer 4, it is enough to use locations 11, 12, and 17 (see subsection about the modelled component) for the position of the actuator within the network (factor M). The excitation frequency (factor N) takes the values of 112 and 198 kHz. The length of the disbond (factor L) is varied from 0 to 10 mm in steps of 5 mm, and from 10 to 50 mm in steps of 10 mm. The total number of cases is 168, with 6 of them corresponding to the baseline states. For each excitation frequency and for each actuator position, the baseline for each actuator-sensor pair corresponds to the case of perfect actuator bonding and no disbond.

The fundamental idea behind this methodology is to model the monitoring environment as accurately as possible, so that a measurement event database can be established numerically, and not experimentally. However, numerical results are purely deterministic and cannot be used directly for statistical analysis. Therefore, a pseudo-stochastic nature is attributed to the DI values by following an approach similar to that used by Memmolo *et al*. [16]. The final DI value, DI_{stoch}, is equal to the DI directly calculated from the numerical data, DI_{num}, plus a random perturbation which depends on a normally distributed relative error, e, as defined in Equation (1).

The normal distribution $e \sim N(\mu, \sigma^2)$ has mean value of zero ($\mu = 0$) and is truncated so that the standard deviation, σ, is bounded by a predefined maximum. Since the adopted DI is the same as that used by Janapati *et al*. [17] (see Equations (2) to (4), where N_{ref} and N_{dmg} are normalised version of the signals in the baseline and damaged conditions, S_{base} and S_{dmg}, respectively), the maximum σ is set equal to 13.27%, as that is the sum of the DI deviations observed by them. In this way it is possible to account for variability factors A-C, O, P in the reliability analysis. The pseudo-stochastic transformation is applied 20 times to each of the 162 non-baseline cases, without discarding the original value, thereby generating a total of 3402 distinct DI values for each of the 7 actuator-sensor pairs.

$$DI_{stoch} = DI_{num} \pm \left(e \cdot DI_{num} \right) \tag{1}$$

$$N_{dmg} = \frac{S_{dmg}}{\sqrt{\sum S_{dmg}^2}} \tag{2}$$

$$N_{ref} = \frac{S_{base} \cdot \sum \left(S_{base} \cdot N_{dmg} \right)}{\sum S_{base}^2} \tag{3}$$

$$DI = \sum \left(N_{dmg} - N_{ref} \right)^2 \tag{4}$$

The resulting DI mean value for the scenario with perfect actuator bonding and damage level just below the critical size is used for the definition of the detection threshold. In the current research the critical disbond size is set to 20 mm, which means the initial threshold value is based on the 10 mm damage cases. The threshold value is then made equal to a multiple of the DI standard deviation. To compute the ROC, fractional multipliers of 0.1, 0.25 and 0.5, and integer multipliers of 1, 3, 5, and 10 are employed in order to obtain different threshold levels. Finally, hit-miss data is generated for each threshold, for each actuator-sensor pair in all simulated cases, which in turn allows the computation of the PoD values. For each damage size greater than zero, PoD is equal to the ratio between the number of hits and the total number of DI values in that damage group. Having performed all the operations for the entire transducer network, the overall PoD of a certain damage size for the entire SHM system is taken as the maximum PoD value among all the actuator-sensor pairs.

NUMERICAL MODELLING

The shape, dimensions and material properties of the modelled structure are inspired by a section of a torsion box panel of a horizontal stabilizer made entirely of carbon fibre reinforced thermoplastic polymer. The adopted symmetric 8-ply stacking sequence was selected such that the difference in laminate stiffness between the model and the original would be minimal. The modelled component is formed by the six stringers and two ribs, as depicted in Figure 1. The main dimensions of the assembly are 790 × 996 mm^2, with the thickness of the structural elements ranging between 3

and 3.5 mm. The simulated damage corresponds to a scenario considered as critical by the manufacturer, where a disbond of the fourth stringer occurs (see Figure 1) due to peel forces caused by the panel deformation after a low-energy impact (~ 50 J) on the same stringer, near the support of rib 2, on the outer side of the panel (see View C of Figure 1). The disbond grows from the impact point towards the rib support. The transducer network is formed by 8 PZT patches distributed as shown in Figure 2.

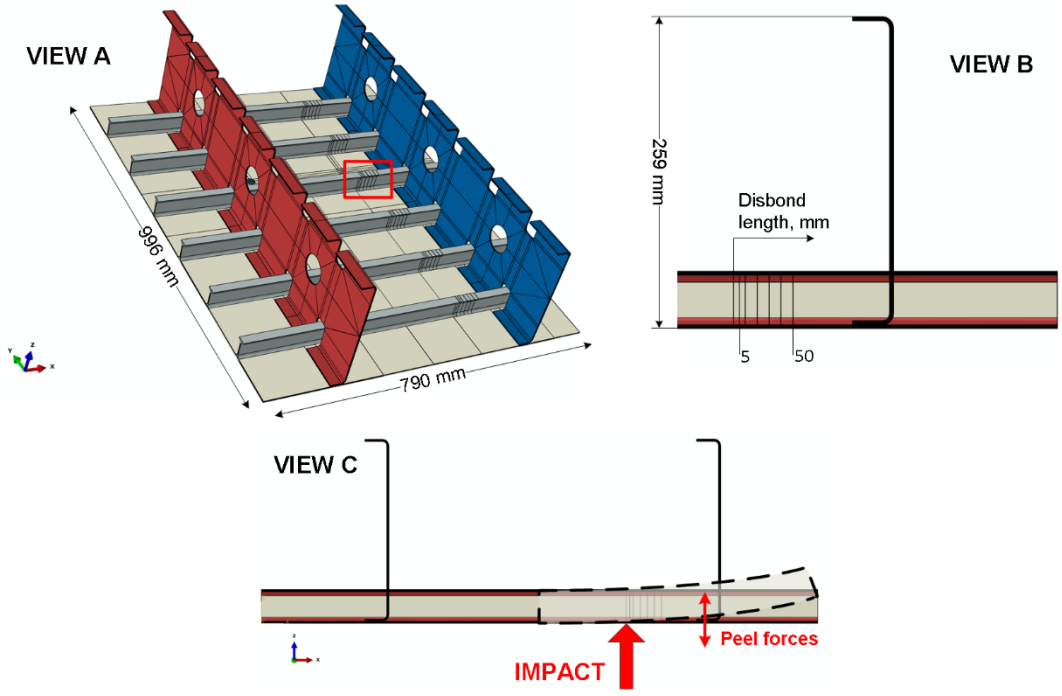

Figure 1. View A – Full model, with the panel, stringer (1 to 6 along Y direction), rib 1 (left side) and rib 2 (right side). Damage (disbond) location indicated by red rectangle. View B - Detail of the disbond area near the support of rib 2. View C - Diagram of the impact and resulting peel forces.

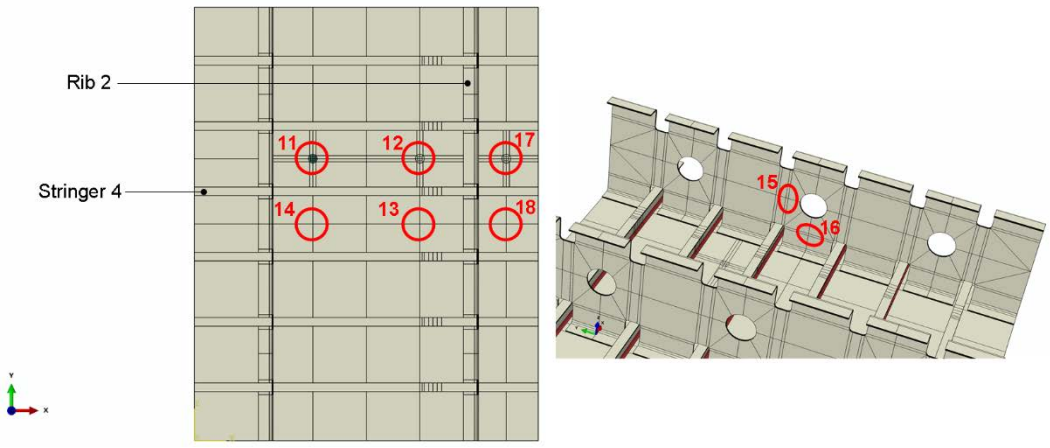

Figure 2. Positions of PZT transducers on the model.

Abaqus/Explicit was used to build an FE model of the torsion box section assembly. All the regions were defined as deformable 3D volumes. The composite material of the individual parts was modelled as anisotropic homogenous, with the nine engineering constants (elastic moduli and Poisson's ratios) defined as by the manufacturer of the original torsion box. The PZT actuator patch was modelled as an orthotropic homogeneous material, with elastic properties equal to those of APC International APC 850 [18, 19] with a nominal diameter of 20 mm and a thickness of 0.4 mm. The actuator bonding layer was assumed to be infinitesimally thin. The mesh was formed by C3D8R elements. In order to respect the Courant-Friedichs-Lewy condition [20], it was ensured that there are five elements per wavelength of A0 Lamb mode [21, 22], which in turn allows for approximately twenty elements per wavelength of S0 Lamb mode, at the centre frequency of excitation. Eight elements were defined along the thickness of the parts (i.e. each composite ply is one element thick), and one element along the thickness of the PZT patch. The mesh controls for each part were defined to achieve the highest mesh quality is achieved while keeping the total number of elements as small as possible. The excitation load was introduced by applying distributed radial forces on the cylindrical face around the perimeter of the actuator patch, according to the PZT force model [23]. The value of those forces was computed based on the constitutive equations of piezoelectricity, for an excitation tone-burst amplitude of 50 V, modulated by a 5-cycle Hanning window. The ultrasonic response was taken from the total displacement of the nodes associated with the sensing positions [24]. The undamaged connections between regions are ensured by tie constraints. The disbond damage is modelled by a contact interaction between the fourth stringer and the panel [25 - 27]. The dynamics of the contacting surfaces were defined by the penalty formulation such that they are allowed to slide on each other while not interpenetrating. For the tangential behaviour, a friction coefficient of 0.2 [28] was adopted. For the normal behaviour, overclosure was dealt with by hard contact. The imperfect actuator bonding was modelled according to the same logic, by defining tie constraints between the bonded area portions, and contact interactions between the non-bonded ones. The simulation time-step was automatically defined by Abaqus by checking the stability condition element by element. The total simulated time interval was defined such that the distance covered by the wavefront of the slowest mode at the centre frequency of excitation is approximately 1 m.

RESULTS AND DISCUSSION

It is first important to verify the results without the variation of the actuator bonding condition. For the purpose of this discussion the focus is placed on the actuator-sensor pair 11-13, and on threshold equal to the triple of the initial value. The PoD curves for that transducer pair at 112 and 198 kHz are depicted in Figure 3a). Damage sizes equal to and beyond the critical value have PoD of more than 80% at 112 kHz and around 60% at 198 kHz. These values differ for each transducer pair, since each relative sensing position is differently affected by the change in the scattering induced by the disbond. In any case, it is possible to observe that the system is more sensitive at 112 kHz than at 198 kHz. This is due to lower DI values at 198 kHz than at 112 kHz, which in turn might mean that the interaction of guided modes

with the disbond at 198 kHz is weaker than at 112 kHz due to the shorter wavelength. The overall PoDs of the critical disbond, for perfect actuator bonding, for the entire SHM network are 1.0 and 0.65, for 112 and 198 kHz, respectively, with both values coming from the transducer pair 11-12.

Looking now at the ROC of transducer pair 11-13 at both 112 and 198 kHz in Figure 4, it is possible to identify two distinct points where the PoD of a 20 mm disbond can be maximised. For 112 kHz the maximum corresponds to a threshold equal to 3 times the initial value, while for 198 kHz, the maximum corresponds to the initial value (note that the initial threshold value is equal to the DI mean for the scenario with perfect actuator bonding and damage size equal to 10 mm). This shows that the SHM system can (at least in theory) have a dynamic threshold definition, capable of adapting the detection level to the operation at multiple excitation frequencies in order to achieve a certain minimum PoD of the critical damage size.

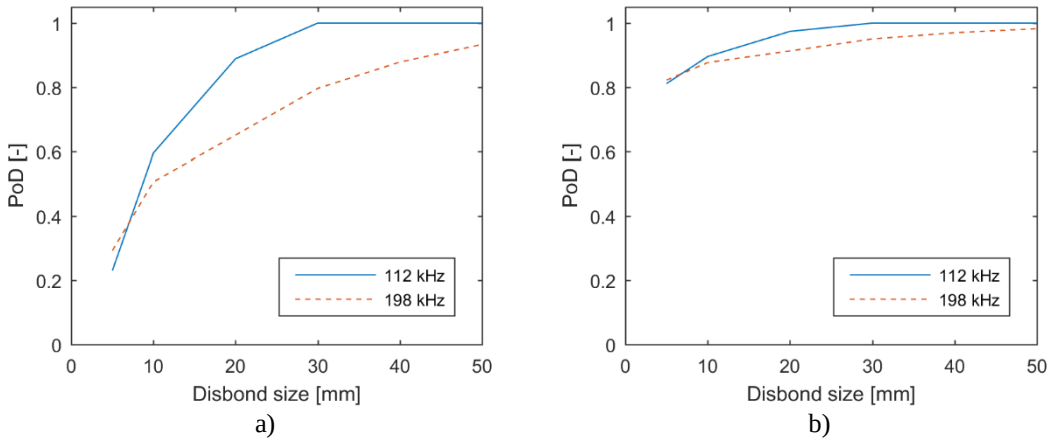

Figure 3. PoD curves for actuator-sensor pair 11-13 at 112 and 198 kHz, a) with perfect actuator bonding, and b) with effect of actuator bonding included.

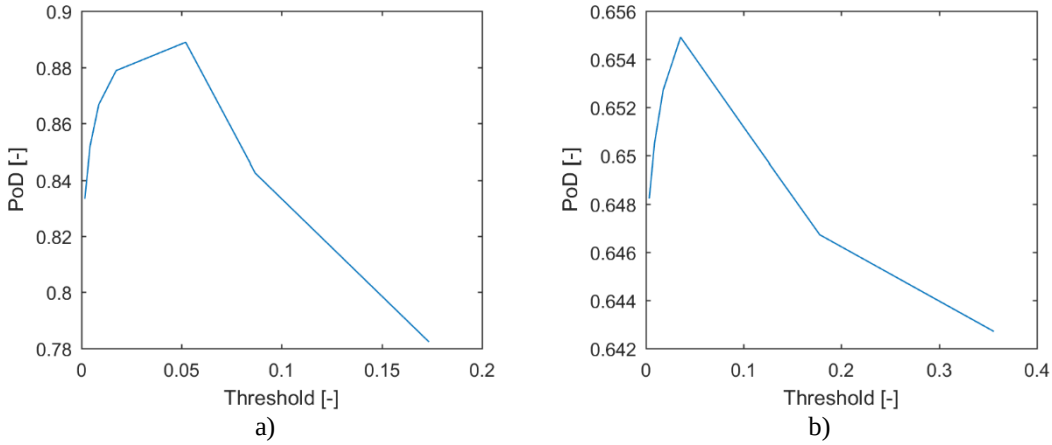

Figure 4. ROC curves from actuator-sensor pair 11-13 for 20 mm disbond and perfect actuator bonding, at a) 112 kHz, and b) 198 kHz.

When the effect of varying actuator bonding is included, the DI greatly increases for the non-critical damage sizes, due to the fact that GW scattering changes induced by the imperfect actuator bonding are comparable to those induced solely by damage, as illustrated in example Figure 5 where the DI values from transducer pair 11-13 are plotted for all the 21 cases. At 112 kHz, with perfect actuator bonding (Figure 5a)), DI values are clustered according to the different damage sizes, while with actuator bonded area equal to 0.75 of the total surface (Figure 5 b)) that is no longer the case. As a result, the PoD of disbonds below 20 mm increases to more than 80% for actuator-sensor pair 11-13, at both 112 and 198 kHz, as shown in Figure 3b). In other words, in the presence of the effect of actuator bonding degradation, the probability of false positives (i.e. detections of non-critical damage sizes) increases greatly. This situation could result in excessive down time of the aircraft. Nevertheless, that same DI magnifying effect is also felt on the critical damage levels, with a 20 mm disbond being detectable more than 90% of the times by transducer pair 11-13. It can be argued that the model of the actuator bonding degradation may not be the most accurate, but it certainly is conservative and thereby lies on “the safe side”. Therefore, the analysis performed with the inclusion of this variability clearly shows how detrimental for the SHM system performance that the bonding factor is, and how important it is to take it into account for the reliability assessment.

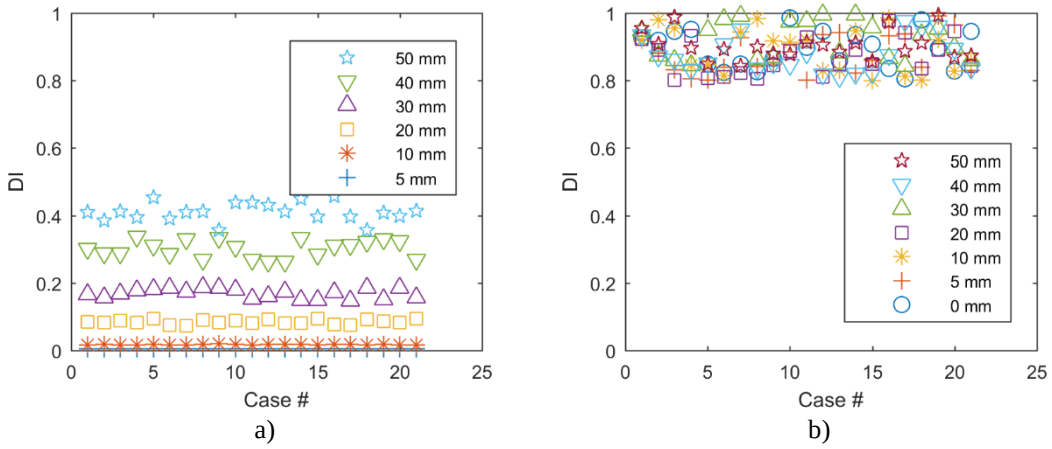

Figure 5. DI values for all cases from actuator-sensor pair 11-13 at 112 kHz, for a) perfect actuator bonding, and b) 25% reduction of actuator bonded area (0 mm is the undamaged state). Note that there are no points for 0 mm in Figure 5a) because those cases correspond to the baseline scenario and are used to compute the DI itself.

CONCLUSIONS

This study focused on improving the characterisation of ultrasonic GW based SHM systems in representative environments for the future commercial aircraft fleet. A full-scale stiffened-panel of a horizontal torsion-box entirely made of carbon fibre reinforced thermoplastic was taken as a case of an aircraft primary structure with material and geometric complexity. The damage scenario was a disbond between a stringer and the panel. A fully computational protocol was developed in order to

perform a reliability assessment of the SHM network. Factors such as size of damage, the excitation frequency, the position of the actuator within the network, and the actuator bonding condition were varied in a finite-element model, enabling the monitoring environment to be simulated in a wide range of scenarios. Damage index values were calculated with the generated numerical responses and artificially disturbed by a pre-defined error, thereby allowing hit-miss data to be generated.

It was theoretically demonstrated that ultrasonic GW based SHM systems are able to detect small disbonds in the complex component studied, even when intra-measurement variability is introduced. More importantly, the study demonstrates the feasibility of quantifying the reliability of such SHM systems solely by computational means. The proposed protocol is not only capable of effectively computing the PoD of the critical damage configuration for a hot-spot in a structure, but also it enables the assessment of performance of the SHM system when actuator bonding degradation is included. In fact, it was observed that a reduction of 25% in the bonded area of the actuator results in a significant increase in the amount of times a non-critical damage is detected, which proves that this variability factor is crucial in improving the robustness of the necessary analysis towards certification of GW based SHM systems.

Additionally, the protocol also allowed the computation of relative operating characteristics of the SHM system, in which the PoD is described as a function of the threshold. In turn, this allowed an analysis of the effectiveness of the selected threshold with varying frequency. It was observed that there is an optimum detection threshold that maximizes the PoD of the critical disbond size at each excitation frequency. Therefore, if monitoring is to be conducted at multiple excitation frequencies, the threshold should be adapted dynamically.

It is important to emphasize that the analysis performed in this study is only possible if the numerical model has been previously validated. Consequently, the proposed protocol does not exclude (on the contrary, it requires) the experimental testing of a few full-scale structural assemblies.

REFERENCES

1. Guo, N. and P. Cawley. 1993. “The interaction of Lamb waves with delaminations in composite laminates”, *J. Acoust. Soc. Am.*, 94(4): 2240-2246.
2. Toyama, N. and J. Takatsubo. 2004. “Lamb wave method for quick inspection of impact-induced delamination in composite laminates”, *Compos. Sci. Technol.*, 64: 1293-1300.
3. Matt, H., I. Bartoli, and F.L. di Scalea. 2005. “Ultrasonic guided wave monitoring of composite wing skin-to-spar bonded joints in aerospace structures”, *J. Acoust. Soc. Am.*, 118(4): 2240-2252.
4. Lu, Y., L. Ye, D. Wang, and Z. Zhong. 2009. “Time-domain analyses and correlations of Lamb wave signals for damage detection in a composite panel of multiple stiffeners”, *J. Compos. Mater.*, 43(26): 3211-3230.
5. Ramadas, C., K. Balasubramaniam, M. Joshi, and C.V. Krishnamurthy. 2010. “Interaction of guided Lamb waves with an asymmetrically located delamination in a laminated composite plate”, *Smart Mater. Struct.*, 19: 1-11.
6. Ng, C.T. and M. Veidt. 2011. “Scattering of the fundamental anti-symmetric Lamb wave at delaminations in composite laminates”, *J. Acoust. Soc. Am.*, 129(3): 1288-1296.
7. Castings, M., D. Singh, and P. Viot. 2012. “Sizing of impact damages in composite materials using ultrasonic guided waves”, *NDT&E Int.*, 46: 22-31.
8. Ochôa, P., V. Infante, J.M. Silva, and R.M. Groves. 2015. “Detection of multiple low-energy impact damage in composite plates using Lamb wave techniques”, *Composites Part B*, 80: 291-298.

9. Dziendzikowski, M., A. Kurnyta, K. Dragan, S. Klysz, and A. Leski. 2016. “In situ barely visible impact damage detection and localization for composite structures using surface mounted and embedded PZT transducers: A comparative study”, *Mech. Syst. Signal Pr.*, 78: 91-106.
10. Wenk, L. and C. Bockenheimer. 2014. “Structure health monitoring: A real-time on-board ‘stethoscope’ for condition-based maintenance”, *Airbus Technical Magazine – Flight Airworthiness Support Technology*, 54: 22-29.
11. *ASM Handbook Volume 17: Nondestructive Evaluation and Quality Control*. ASM International.
12. MIL-HDBK-1823A, *Nondestructive Evaluation System Reliability*, Department of Defense USA, April 2009.
13. Forsyth, D.S. 2016. “Structural health monitoring and probability of detection estimation”, *AIP Conf. Proc.*, 1706(200004): 1-6.
14. Cobb, A.C., J.E. Michaels, and T.E. Michaels. 2009. “Ultrasonic structural health monitoring: a probability of detection case study”, in *Review of Quantitative Nondestructive Evaluation 28*, ed D.O. Thompson and D.E. Chimenti, eds. American Institute of Physics.
15. Cobb, A.C., J. Fisher, and J.E. Michaels. 2009. “Model-assisted probability of detection for ultrasonic structural health monitoring”, in *Proc. of the 4th European-American Workshop on Reliability of NDE*, June 24-16, 2009.
16. Memmolo, V., F. Ricci, L. Maio, N.D. Boffa, and E. Monaco. 2016. "Model assisted probability of detection for a guided waves based SHM technique", *Proc. of SPIE*, 9805(980504): 1-12.
17. Janapati, V., F. Kopsaftopulos, F. Li, S.J. Lee, and F.K. Chang. 2016. “Damage detection sensitivity characterization of acousto-ultrasound-based SHM techniques”, *Struct. Health Monit.*, 15(2): 143-161.
18. Pérez, N., F. Buiochi, M.A.B. Andrade, and J.C. Adamowski. 2012. “Numerical characterization of soft piezoelectric ceramics”, *AIP Conf. Proc.* 1433: 648-651.
19. Giurgiutiu, V. 2014. *Structural Health Monitoring with Piezoelectric Wafer Active Sensors*, 2nd ed. Academic Press-Elsevier, San Diego, California.
20. Courant, R., K. Friedrichs, and H. Lewy. 1967. “On the partial difference equations of mathematical physics”, *IBM J. Res. Dev.* 11(2): 215-234.
21. Drozdz, M.B. 2008. “Efficient finite element modelling of ultrasound waves in elastic media”, PhD thesis, Department of Mechanical Engineering, Imperial College of Science Technology and Medicine, University of London.
22. Blake, R.J. and L.J. Bond. 1990. “Rayleigh wave scattering from surface features: wedges and down-steps”, *Ultrasonics* 28: 214-228.
23. Nieuwenhuis, J.H., J. Neumann, D.W. Greve, and I.J. Oppenheim. 2005. “Generation and detection of guided waves using PZT wafer transducers”, *IEEE Trans. Ultrason., Ferroelect., Freq. Control* 52(11): 2103-2111.
24. Su, Z. and L. Ye. 2005. “Lamb wave propagation-based damage identification for quasi-isotropic CF/EP composite laminates using artificial neural algorithm: Part I – Methodology and database development”, *J. Intell. Mater. Syst. Struct.* 16: 97-111.
25. Kang, K.T., H.J. Chun, J.A Lee, J.H. Byun, M.K. Um, S.K. Lee, and S.K. Byung. 2011. “Damage detection of composite plates using finite element analysis based on structural health monitoring” *Journal of Materials Science and Engineering B* 1: 14-21.
26. Zhang, Z., K. Shankar, M. Tahtali, and E.V. Morozov. 2010. “Vibration modelling of composite laminates with delamination damage”, in *Proc. of the 20th International Congress on Acoustics*, August 23-27, 2010,
27. Garcia D., R. Palazzetti, I. Trendafilova, C. Fiorini, and A. Zucchelli. 2015. “Vibration-based delamination diagnosis and modelling for composite plates”, *Compos. Struct.* 130: 155-162.
28. Schön, J. 2000. “Coefficient of friction of composite delamination surfaces”, *Wear* 237: 77-89.